

# Watertight Robust Osteoconductive Barrier for Complex Skull Base Reconstruction: An Expanded-endoscopic Endonasal Experimental Study

Alhusain NAGM,<sup>1,2</sup> Toshihiro OGIWARA,<sup>1</sup> and Kazuhiro HONGO<sup>1</sup>

<sup>1</sup>Department of Neurosurgery, Shinshu University School of Medicine, Matsumoto, Nagano, Japan;

<sup>2</sup>Department of Neurosurgery, Faculty of Medicine, Al-Azhar University, Cairo, Egypt

## Abstract

Endoscopic skull base reconstruction (ESBR) following expanded-endoscopic endonasal approaches (EEA) in high-risk non-ideal endoscopic reconstructive candidates remains extremely challenging, and further innovations are still necessary. Here, the aim is to study the reconstructive knowledge gap following expanded-EEA and to introduce the watertight robust osteoconductive (WRO)-barrier as an alternative durable option. Distinctively, we focused on 10 clinical circumstances. A 3D-skull base-water system model was innovated to investigate the ESBR under realistic conditions. A large-irregular defect (31 × 89 mm) extending from the crista galli to the mid-clivus was achieved. Then, WRO-barrier was fashioned and its tolerance was evaluated under stressful settings, including an exceedingly high (55 cmH<sub>2</sub>O) pressure, with radiological assessment. Next, the whole WRO-barrier was drilled to examine its practical-safe removal (simulating redo-EEA) and the whole experiment was repeated. Finally, WRO-barrier was kept into place to value its 18-month long-term high-tolerance. Results in all experiments of WRO-barriers were satisfactorily fashioned to conform the geometry of the created defect under realistic circumstances via EEA, tolerated an exceedingly high pressure without evidence of leak even under stressful settings, resisted sudden-elevated pressure, and remained in its position to maintain long-term watertight seal (18 months), efficiently evaluated with neuroimaging and simply removed-and-reconstructed when redo-EEA is needed. In conclusion, WRO-barrier as an osteoconductive watertight robust design for cranial base reconstruction possesses several distinct qualities that might be beneficial for patients with complex skull base tumours.

Key words: skull base reconstruction, endoscopic endonasal approach, CSF leak, transsphenoidal surgery, watertight

## Introduction

The cerebrospinal fluid (CSF) leak rate following expanded-endoscopic endonasal approach (EEA) is still high<sup>1–11</sup> (transclival-EEA: 20–41.2%;<sup>8,9</sup> anterior cranial base (ACB)-EEA = 30%)<sup>1–8,12</sup> and associated with brain deformities.<sup>10</sup> Besides, immediate watertight endoscopic skull base reconstruction (ESBR) remains extremely challenging (Fig. 1) even with available methods.<sup>1–18</sup> Therefore, technological advances and further innovations are needed to improve the reconstructive options.<sup>1–7,10,12</sup> Vascularized flaps (which are superior to avascular dural reconstruction),<sup>3,15,19,20</sup> have changed the history with EEA as

they significantly altered the CSF leak rate; however, these options are not always available (non-ideal endoscopic reconstructive candidates), bounded by some technical restrictions,<sup>3,4,14,20</sup> or more invasive and associated with donor site serious complications.<sup>3,19</sup> Lumbar drain significantly reduces the CSF leak rates,<sup>9</sup> nevertheless, some concerns regarding its indications, the duration and the postoperative meningitis still exists.<sup>21</sup>

By concluding the experiences of ESB experts<sup>1–7</sup> based on a thorough survey of the English literature<sup>8–10,12–16,18,21–31</sup> we were able to study the reconstructive knowledge gap. If there is an available watertight robust barrier that is enough to withstand postoperative adjunctive radiation and chemotherapy (avascular environment), applicable for irregular-deep-critical bone defects, efficiently evaluated with neuroimaging, simple in its technique, without donor site complications and can be considered as a

Received October 30, 2018; Accepted December 17, 2018

Copyright© 2019 by The Japan Neurosurgical Society  
This work is licensed under a Creative Commons Attribution-NonCommercial-NoDerivatives International License.

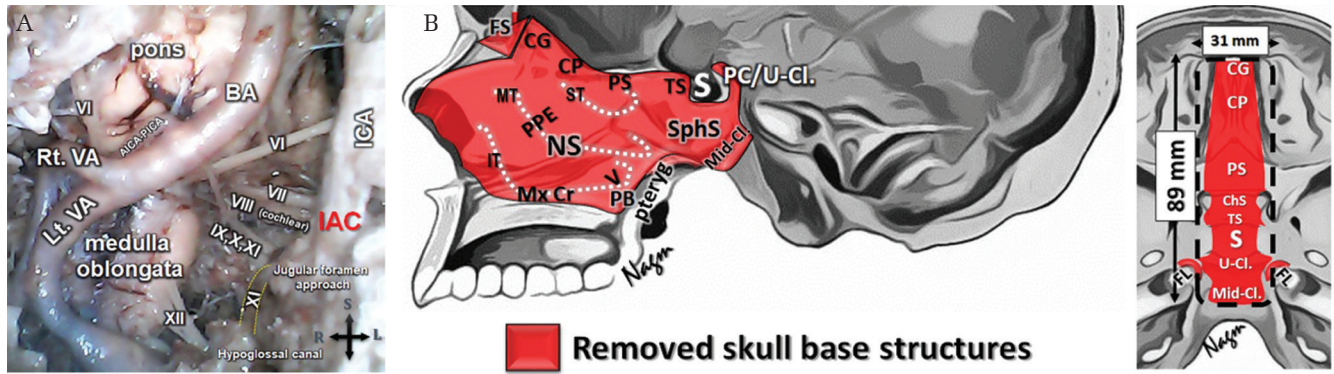


**Fig. 1** (A) Endoscopic video-captured view following cadaveric dissection [by the lead author (AN)]: An example of the daunting challenge of complex skull base defect following extensive drilling of the clivus and completing the left-sided sub-lacerum infrapetrous approach to the jugular foramen. The brainstem, cranial nerves from VI to XII, union of both vertebral arteries to form the basilar artery can be appreciated via endoscopic endonasal perspective. BA: basilar artery, Rt. VA: right vertebral artery, Lt. VA: left vertebral artery; AICA: anterior inferior cerebellar artery, PICA: posterior inferior cerebellar artery, ICA: internal carotid artery, VI: 6th cranial nerve, VII: 7th cranial nerve, VIII: 8th cranial nerve, IX: 9th cranial nerve, X: 10th cranial nerve, XI: 11th cranial nerve, XII: 12th cranial nerve, S: superior, R: right, L: left. (B) The 3D-skull base model (sagittal “left” and axial “right” views) was used to create a 31 × 89 mm skull base defect (*black-dotted line* on axial view) extending from the crista galli (Draf III) to the mid-clivus via EEA. Extensive removal of all turbinates, nasal septum and the maxillary crest were completed for wide exposure, and careful partial skeletonization of the silicon representing the paraclival-ICAs were achieved. FS: frontal sinus (Draf III), CG: crista galli, CP: cribriform plate, PS: planum sphenoidale, ChS: pre-chiasmatic sulcus, TS: tuberculum sellae, S: sella, SphS: sphenoid sinus, PC/U-cl: posterior clinoid/upper-clivus, mid-cl: mid-clivus, FL: foramen lacerum, ST: superior turbinate, MT: middle turbinate, IT: inferior turbinate, PPE: perpendicular plate of ethmoid, NS: nasal septum, V: vomer, PB: palatine bone, Mx Cr: maxillary crest, pteryg: pterygoids.

good endoscopic reconstructive alternative, it will be a great advantage. We selected a well-known malleable osteoconductive-and-osteoinductive material,<sup>32–36</sup> which became a robust barrier within a few minutes, that have good biocompatibility, superior bone regeneration and can survive in avascular environment.<sup>33,34</sup> Herein, we present the watertight robust osteoconductive (WRO)-barrier for ESB as an alternative durable option and we will discuss its distinct qualities and limitations.

## Materials and Methods

The idea, design, and the whole experiment (Fig. 2) was performed by the lead author (AN) with endoscopic 2-hand technique. The diagnosis of negative/positive leak was done clinically by three independent neurosurgeons. The radiological 3D-WRO-barrier’s configuration and reconstruct-defect subtraction images were designed by independent radiological-technicians who are completely blinded to the whole study.

### IRB/ethics committee statement

After qualification as exempt status by the IRB guidelines this *in vitro* experimental study, which

based on 3D-phantom skull base models, was conducted.

### Inclusion criteria

As a novel of this study, we focused on 10 real (stressful) conditions, first, considering the most difficult defects (clivus)<sup>1–7</sup> that have significant depth, challenging 3D-geometry [paraclival internal carotid artery (ICA)] and high-flow CSF (prepontine cistern) (Fig. 1); second, deep-narrow and wet endoscopic field (Fig. 3); third, large defect (from anterior-to-posterior fossae) with irregular bony framework (challenging sloping angles) (Figs. 1 and 3); fourth, tailorable reconstructive material with clinical evidence (bone paste); fifth, dynamic settings (simulating the postoperative patient handovers/daily activity); sixth, suddenly elevated H<sub>2</sub>O pressure (simulating sudden/unexpected increase in the intracranial pressure (ICP): cough, sneezing); seventh; relatively little biological reaction in the early postoperative period; eighth, avascular reconstructive-bed (postoperative adjunctive chemo-radiotherapy)<sup>33,34</sup>; ninth, redo-EEA for recurrent-or-staged tumor surgery; and tenth, ARTCEREB (Otsuka Pharmaceutical Factory, Inc., Tokyo, Japan) as a CSF-substitute,<sup>37</sup> instead of water, to simulate the real intraoperative wet condition that

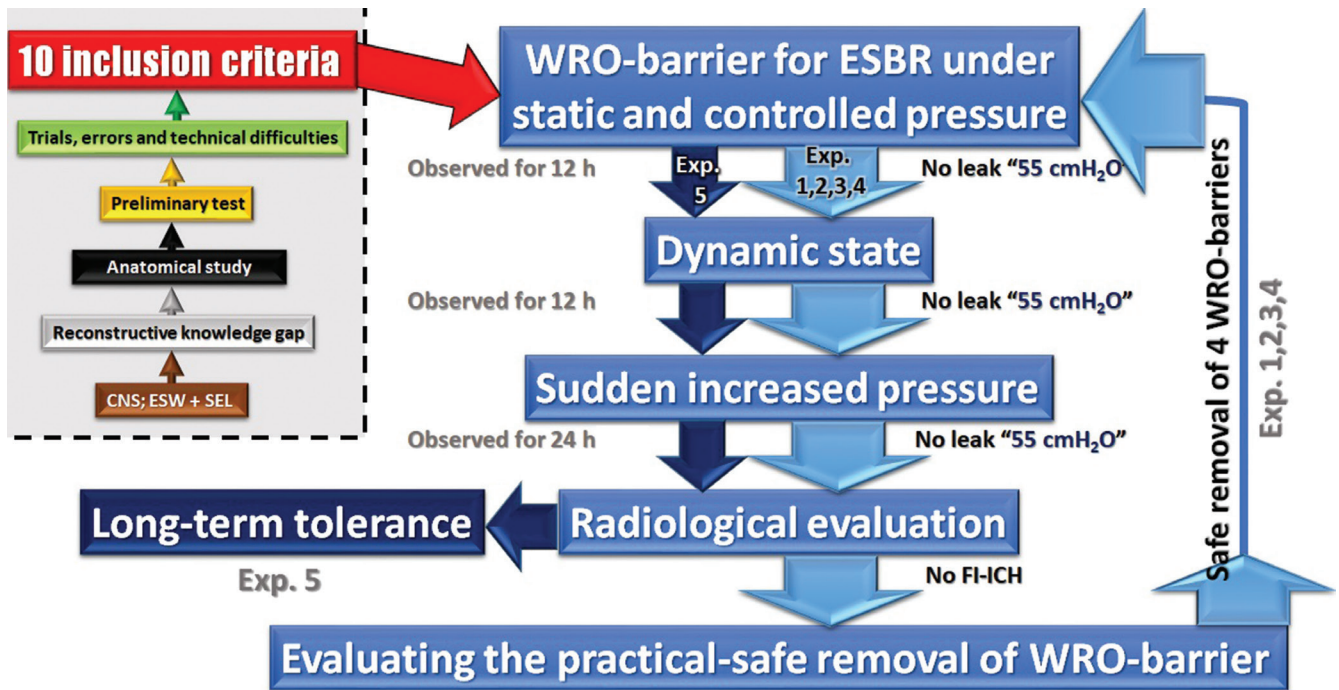


Fig. 2 Study overview. *Broken black line (grey background)*: Pre-experimental stage. By concluding experts' experiences based on a thorough survey of the English literature (*brown box*), we were able to identify the reconstructive knowledge gap (*gray box*). Besides, following anatomical study (*black box*), preliminary test (*orange box*), many trials and errors (*green box*), we included 10 inclusion criteria (*red box*) to be evaluated in the experiments (total of five: *light-blue and dark-blue arrows*). Watertight robust osteoconductive (WRO)-barriers were created and evaluated under static settings with gradual increased pressure (55 cmH<sub>2</sub>O) and observed to diagnose positive/negative leak. No evidence of leak in all experiments under static or dynamic settings. No evidence of CSF-leak following sudden pulse pressure. The radiological evaluation confirmed ideal WRO-barriers' configurations in all five experiments. Practical-safe removal followed by reconstruction of WRO-barriers were achieved successfully (*light-blue pathway*). Following the last experiment (number = 5), WRO-barrier was kept into place to evaluate its long-term tolerance (*dark-blue pathway*). CNS: Congress of Neurological Surgeons, ESW: Endoscopic series webinars (2016–2017),<sup>1–7</sup> SEL: a thorough survey of the English literature, WRO: watertight robust osteoconductive, ESBR: endoscopic skull base reconstruction, Exp.: experiment, FI-ICH: fashioning-induced intracranial herniation.

might have specific (biochemical/physical) contributing effect, and we added red-color to accurately diagnose the leakage point.

## Experiments

A specially made 3D-skull base-water system model (with injected silicon representing the pertinent neurovascular structures) was innovated to investigate the ESBR under realistic circumstances (Figs. 1B, 2–5A and 5B). From the cranial side a tailored water-system, that accommodates 55 cmH<sub>2</sub>O, was directly attached to the outline of the defect (Figs. 3 and 4).

First (defect); the 3D-skull base model<sup>38,39)</sup> was used to create a 31 × 89 mm (Fig. 1B) skull base irregular-defect including ACB resection and extending to-the mid-clivus via EEA with careful skeletonization of the silicon representing the paraclival-ICA (Fig. 3) based on the University of Pittsburgh Medical Center (UPMC) Anatomical Dissection Guideline.<sup>40)</sup> Second (watertight-barrier); initially, wet

endoscopic field<sup>28)</sup> was created (Fig. 3). Then, the skeletonized paraclival-silicon/ICA were protected with bridge-tailored Goretex sheets (Fig. 4B). The defect was filled with INTEGRAN (Mississauga, Canada) sheets (0.5 g, 45 × 30 mm<sup>2</sup> and 0.2 g, 200 × 50 mm<sup>2</sup>) and a tailored Goretex sheet (larger than the defect) was used as a protective inlay layer to avoid intracranial reconstruct-migration. A total of 12 mL osteoconductive paste (OP) (BIOPEX-R: HOYA Technosurgical Co., Tokyo, Japan) was prepared for injection in an S-shaped manner (Fig. 5A) and homogeneously fashioned to conform the geometry of the defect under direct endoscopic control. Then, 5 mL of fibrin glue was applied over the whole osteoconductive paste including its edges to ensure complete sealing of any invisible tiny channels<sup>1–7,14,19,20,22,41)</sup> and to create the WRO-barrier.

Third (stressful settings); to evaluate the initial/static tolerance of the WRO-barrier, ARTCEREB was allowed to continue to fill the cylinder gradually



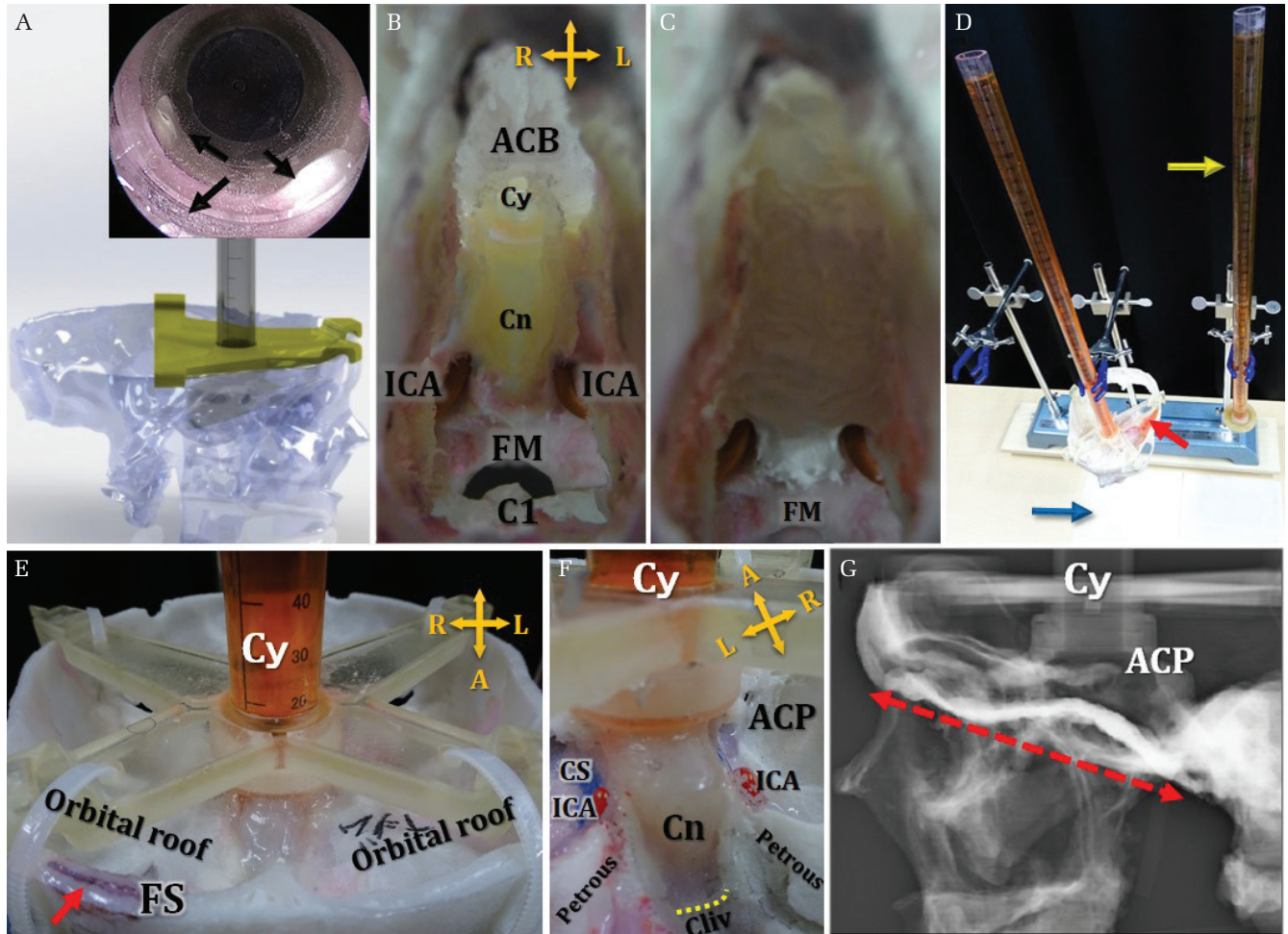


**Fig. 3** Water-system and pertinent anatomy: (A) Control: Transparent 3D-skull base model (an identical 3D-copy of our innovated opaque model) used to practice ESBR under both endoscopic and direct visual control. This control allowed us to understand our technical difficulties and perform many trials before proceeding to our experiment. *Upper right inset*: Wet endoscopic field (via EEA) was created with ARTCEREB under slow continuous dripping (1 cm/10 s) along the inner wall of the cylinder (*black arrows*). (B) Macro-photograph via the nose “submento-vertical view” showing the skull base defect (extending from anterior-to-posterior cranial fossae) continuing to the inner space of the conduit and the cylinder. (C) The osteoconductive paste covering the whole defect in B. (D) WRO-barrier tolerates an exceedingly high pressure (55 cmH<sub>2</sub>O) without evidence of leak (dry filter paper “*blue arrow*”) even under stressful settings. Control: The simple sellar model (*yellow arrow*) also tolerates the same settings. Notice the red stain around the left petrous bone (*red arrow*): previous amended error (back-pressure leak from the petrous bone due to exceedingly high water pressure). All errors were amended and excluded from the index study. (E and F) Pertinent anatomy of anterior-(E) and-(F) middle-posterior cranial fossae in relation to the defect. The *yellow-dotted line* (F) shows the lower limit of our clival drilling. *Red arrow* (E) indicates an “error”: sealed leak from the pneumatized frontal sinus (back-pressure leak due to exceedingly high water pressure). All errors were amended and excluded from the index study. In order to accommodate the irregular geometric borders of the defect, a specially made 3D-plastic cone-like conduit was directly attached to the outline of the defect. Then a plastic cylinder, was attached to the top of the conduit. (G) Plain X-ray lateral view of the reconstructed 3D-skull base model showing WRO-barrier’s shape and position (*double-head red arrow* indicates the extent of the defect/reconstruction). ACB: anterior cranial base, Cy: cylinder, Cn: conduit, ICA: internal carotid artery, FM: foramen magnum, C1: first cervical vertebra, FS: frontal sinus, CS: cavernous sinus, ACP: anterior clinoid process, Cliv: clivus, A: anterior, R: right, L: left.

till its leakage (to define the H<sub>2</sub>O-level at leakage), or up to a maximum of 55 cmH<sub>2</sub>O and observed for 12 h (Figs. 4 and 5). To assess the stability of WRO-barrier under dynamic state, significant random

motions (including transportation to the radiology department) was applied to the model and leakage was observed for another 12 h. To examine the effect of sudden increased ICP, first; 40-cm fluid was

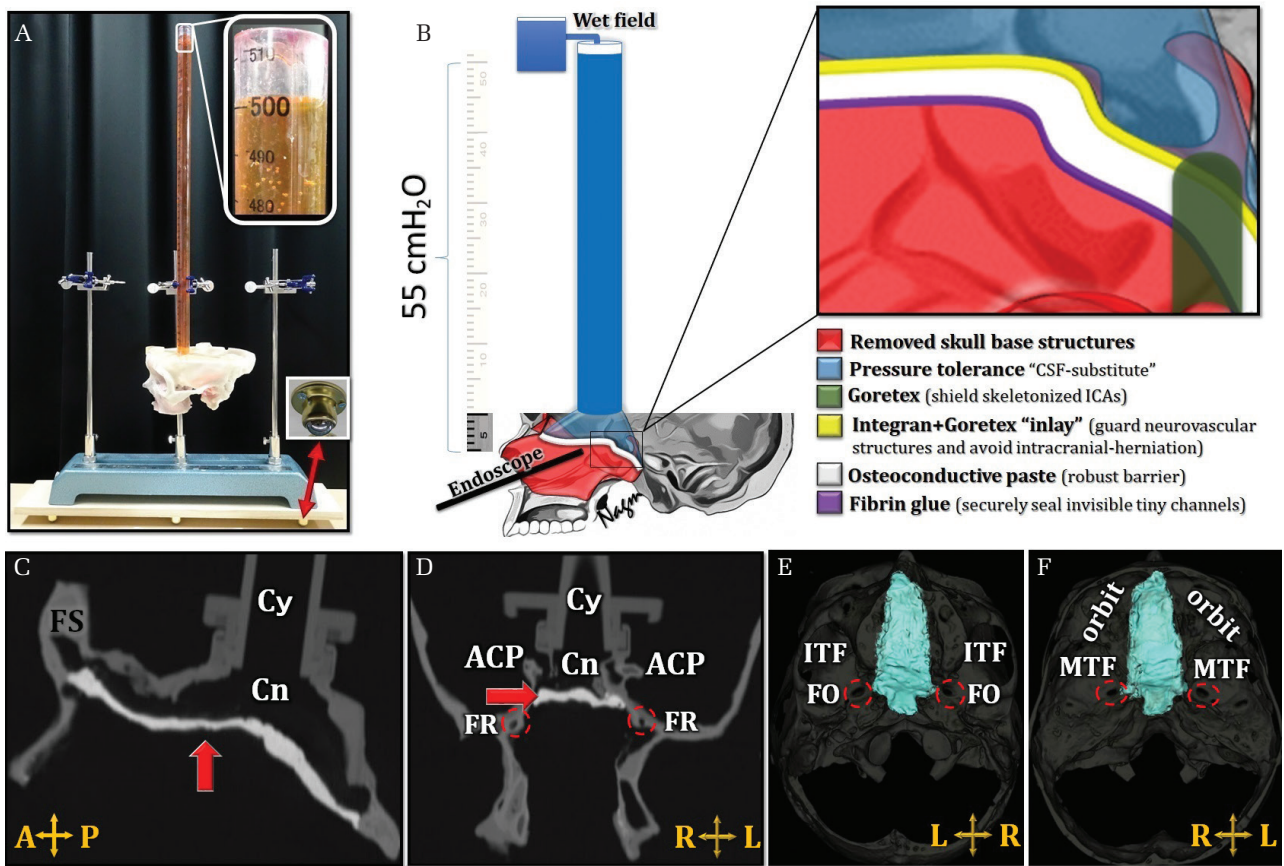


**Fig. 4** Watertight robust osteoconductive (WRO)-barrier for endoscopic skull base reconstruction. (A and B) WRO-barrier tolerates an exceedingly high pressure of 55 cmH<sub>2</sub>O (50 cm H<sub>2</sub>O in cylinder “upper inset” + 5 cm H<sub>2</sub>O in conduit “B”) without evidence of leak even under stressful settings (*double-head arrow* indicates the wheels “lower inset” that used in dynamic settings). Magnified view of WRO-barrier (B) that used to reconstruct a large skull base defect (*red*) via EEA through a deep-narrow-critical wet (*blue*) endoscopic field. Goretex sheet shielded skeletonized paraclival-carotids (*green*), Integran + Goretex “inlay” guard neurovascular structures and avoid intracranial-herniation (*yellow*), osteoconductive paste as a robust barrier (*white*) and fibrin glue securely seal invisible tiny channels (*violet*). (C and D) CT studies (sagittal C and coronal D images) indicates the defect/ approach and the ideal shape-and-position of WRO-barrier (*red arrows*). The vidian-rotundum (foramen rotundum = *red circle*) line was identified in the coronal plane. The vidian canal was extensively drilled (scarified imaginary vidian nerve). E and F) 3D-CT study showing the configuration of WRO-barrier (*blue*) via the extracranial (E)-and-intracranial (F) prospective. Cy: cylinder, Cn: conduit, FS: frontal sinus, ACP: anterior clinoid process, FR: foramen rotundum, FO: foramen ovale, ITF: infratemporal fossa, MTF: middle cranial fossa, A: anterior, P: posterior, R: right, L: left.

drained cranially to maintain normal CSF pressure (15 cmH<sub>2</sub>O), then the model was rapidly re-filled with one-pulse 40-cm-ARTECERB (total 55 cmH<sub>2</sub>O), and leakage was observed for another 24 h.

Fourth (neuroimaging); plain X-ray (Fig. 3), 3D-computed tomography (CT) (Figs. 4C–4F and 5B) and magnetic resonance imaging (MRI) were done to evaluate the WRO-barrier’s configuration. Fifth (recurrence and long-term); the whole WRO-barrier was drilled via EEA to assess its practical-safe removal (when redo-EEA is needed) (Fig. 5) and reconstructed again following the same principles. The whole experiment was repeated five times (Fig. 2). Following the

final (5th) reconstruction, the WRO-barrier was kept into place for 18 months (the maximum time needed for sufficient osteo-angiogenesis is 10 months)<sup>32,35,36,42</sup> to evaluate its long-term tolerance under 55 cmH<sub>2</sub>O.

## Results

### Endoscopic use

Watertight robust osteoconductive-barrier was meticulously applied via EEA and homogenously fashioned to conform the challenging geometry of the large 3D-skull base model’s defect (Figs. 3–5) under realistic circumstances (deep-narrow, wet and



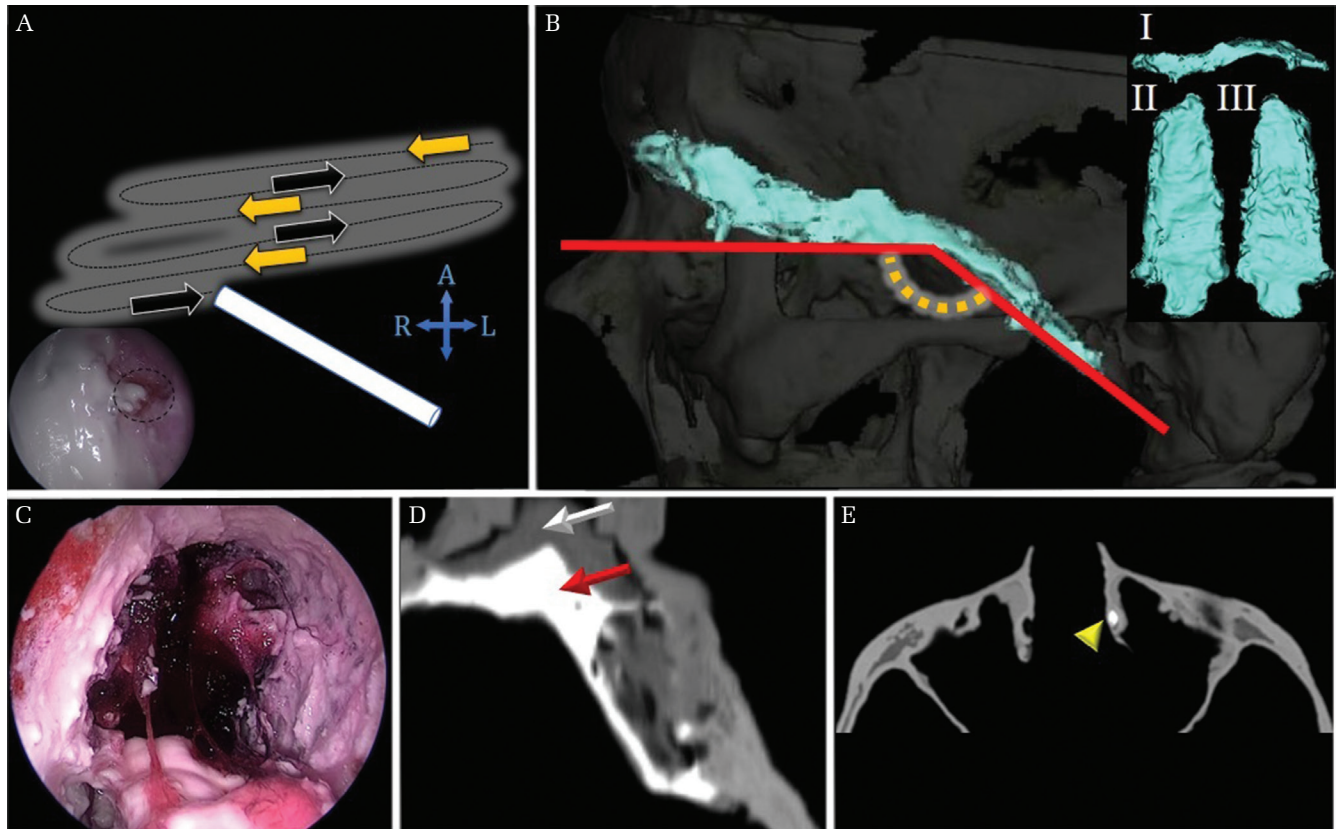


**Fig. 5** How to avoid complications: Risk of fashioning-induced intracranial herniation or migration. (A) Injecting the osteoconductive paste in an S-shaped manner (*yellow-and-black arrows*) can homogeneously fashion the defect. An endoscopic view (inset) showing the homogeneously-fashioned WRO-barrier with a special care to include all leaking points (*black circle*). (B) Ideal WRO-barrier's configuration (*blue*) from different prospective (I: lateral, II: intracranial-and- III: extracranial-views). The transition angle (*yellow dotted-curved line*): between the horizontal line representing the ACB, and the oblique line representing the middle-and-posterior cranial fossae (*red lines*) where an easy-but-dangerous manipulative force is more likely to occur. (C–E) Pre-experimental trials and errors. (C) Removal of WRO-barrier: endoscopic view (rigid 4 mm in diameter, 18 cm in length, with angled lens (30°): Karl Storz, Tuttlingen, Germany) showing fashioning-induced intracranial herniation at the transition angle. Notice the absence of Goretex sheet makes the imaginary neurovascular structures at a great risk. (D) CT sagittal view (300% magnification) showing dangerous WRO-barrier's configuration. Intracranial herniation of the paste (*red arrow*) and the inlay materials = Spongcel (*white arrow*). (E) CT axial view showing the escape of the paste along the left lacrimal duct (*yellow arrow-head*). A: anterior, R: right, L: left.

critical operative field) in all experiments (number = 5). No evidence of critical intracranial fashioning-induced herniation in all experiments.

#### Stressful settings' tolerance, neuroimaging, removal and reconstruction

In all experiments WRO-barrier withstands an exceedingly high pressure (55 cmH<sub>2</sub>O) under static/dynamic settings (Fig. 4) without evidence of leak, and tolerated sudden-pulse pressure. Additionally, remained in its position to maintain watertight seal even under stressful settings in all experiments, efficiently evaluated with neuroimaging (MRI-compatible), simply removed and reconstructed when redo-EEA is needed.

#### Long-term tolerance

Watertight robust osteoconductive-barrier never destroyed by CSF-substitute (18-month long-term tolerance). The abovementioned values are considered as distinct qualities for WRO-barrier.

## Discussion

#### Reconstructive knowledge gap and the advantages of WRO-barrier

*In vitro* tolerance of the reconstructive materials might differ under real applications<sup>8–10,12–16,18,21–31</sup> and an innovative experimental study that mimicking clinical circumstances might be helpful, chiefly for high risk<sup>21</sup> and non-ideal endoscopic reconstructive patients who

underwent expanded-EEA. From this point of view, while taking into consideration the risks of rigid reconstruction, we included 10 realistic circumstances to avoid the gap between *in vitro* experiments and real clinical tolerance<sup>8–10,12–16,18,19,21–31</sup> and to overcome some technical restrictions.<sup>1–7,13,16,19,20</sup> The malleable osteoconductive paste<sup>32–36</sup> was selected as it can be simply fashioned during its endoscopic application for challenging skull base defects, converted to a watertight robust barrier within a few minutes and efficiently evaluated with neuroimaging. This injectable paste promotes epithelialization and complete bone healing within 10 months,<sup>32–36,42</sup> therefore we took into consideration this postoperative period and we evaluated the 18-month long-term tolerance of WRO-barrier. During this 18-month period, there were neither evidence of cracks/fractures within the barrier, nor CSF leak.

The OP can act as a drug-carrier<sup>35</sup> for radioactive particles,<sup>33</sup> and can be loaded with controlled release system of antibiotics (gentamicin, vancomycin),<sup>35</sup> therefore, WRO-barrier can survive in avascular environment induced by postoperative adjunctive radio/chemotherapy.<sup>33,34</sup> Besides, the WRO-barrier can resist infection by its high antimicrobial potency.<sup>35</sup> In real clinical application, we can replace the protective inlay Goretex sheet by fascia lata graft (natural layer) as an additional defensive measure against infection.

### Technical difficulties: how to overcome

Before our experiment, we did a preliminary test with many trials and errors in order to understand our technical difficulties. Previously, we faced a risky WRO-barrier's configuration with fashioning-induced intracranial herniation (FI-ICH) (Figs. 5C and 5D) associated with CSF leak in 20% (tolerance pressure decreased from 55 to 42 cmH<sub>2</sub>O “very high pressure”). Besides, noticed paste migration via the injured nasolacrimal duct (Fig. 5E). We realized that such risk of FI-ICH was attributed to the so called transition angle (Fig. 5B) at the central skull base (junction between the anterior cranial fossa and clivus). This transition directly faces the main surgical axis of the EEA, where our lead author (AN) heavily applied the OP to cover the central skull base defect, then started to fashion the barrier over the clival defect followed by the ACB defect. In the index experiment, we have amended this problem by injecting the OP in an S-shaped fashion (Fig. 5A) starting from the ACB defect, followed by the central and finally the clival defects. We included the inlay Goretex sheet for additional protection.

Clinically, WRO-barrier could be created under intraoperative radiological guidance (fluoroscopy

or CT) (Figs. 3–5). This will be very helpful to homogeneously and safely fashion the OP based on direct endoscopic control and obvious radiological reference. Additionally, some reactive membranes<sup>41</sup> that prevent OP-leakage might be useful.

### Why a single 3D-skull base model?

The purpose of repeating the experiment five times while using a single skull base model was to simulate the redo-EEA/staged-surgery. And once we got satisfactory results, further repetitions were discontinued to focus on long-term tolerance.

### Limitations and exceptional concerns

Watertight robust osteoconductive-barrier might be extremely beneficial for designated patients with large skull base defect and high-flow CSF leak following aggressive resection for complex tumour that require postoperative radio/chemo-therapy, and associated with multiple risks.<sup>1–7,21</sup> This WRO-barrier is not exothermic, so no heat-related injuries to the surrounding critical structures. However, we are aware that bony framework seems to be an indispensable prerequisite to hold the whole WRO-barrier into place. Therefore, such kind of reconstruction cannot be considered as a standard solution following all expanded-EEAs.

Additionally, despite our lead author (AN) paid every effort to innovate realistic settings [including materials with clinical evidence under wet endoscopic field to reconstruct the most challenging skull base defect (Fig. 1)] to avoid any possible different reaction between *in vitro* experiments-and-real (*in vivo*) clinical tolerance, we believe that a well-controlled clinical trial is required to understand how the WRO-barrier works in the human biological circumstances. To be reasonable, the *in vivo* WRO-barrier reconstruction should be carefully evaluated for less puzzling defects before facing the daunting challenge (Fig. 1).

Based on our results, WRO-barrier possesses several distinct qualities that can change the CSF leak rate. Although we successfully created a high-tolerance barrier (55 cmH<sub>2</sub>O) with an ideal configuration in the index experiment (Figs. 3G and 5B–5F), our pre-experimentally documented risk of herniation (Figs. 5C–5E) should be taken into consideration before clinical application. Such risk was addressed successfully after proper understating. Therefore, we did not encounter the same problem in the index experiment.

In our study we selected non-ideal reconstructive candidates, accordingly our results are not comparable with failure rate and current standards for EEA using vascularized flaps.

In addition, our novel experimental study under realistic environment might open the door for similar researches and stimulates further innovations.

## Conclusion

Watertight robust osteoconductive-barrier as an osteoconductive watertight robust design for endoscopic cranial base reconstruction can contribute in decreasing the CSF leak rate and can be considered as a promising alternative durable option for designated patients with complex/invasive skull base tumours that require aggressive removal (with large defect) and postoperative adjunctive chemo-radiotherapy (avascular environment). It tolerates an exceedingly high (55 cmH<sub>2</sub>O) pressure and remains in its position to maintain watertight seal even under stressful conditions. Besides, it can be simply removed and reconstructed when redo-surgery is needed.

## Author Contributions

- The idea, design, anatomical dissection, preliminary test, trials, studying the reconstructive knowledge gap and the whole experiment was performed by the lead author (AN) with endoscopic 2-hand technique. Interactively attending the Congress of Neurological Surgeons; Endoscopic series webinars 2016–2017: AN. Contacting endoscopic skull base experts: AN. Conclude experts' experiences to identify the knowledge gap: AN. Did the diagnosis of CSF leak (negative/positive) radiological assessment: AN, TO and KH. The acquisition, analysis and interpretation of data: AN.
- Drafting the work: AN, Revising it critically for important intellectual content: AN, TO and KH.
- Final approval of the version published: AN, TO and KH.
- Agreement to be accountable for all aspects of the work in ensuring that questions related to the accuracy or integrity of any part of the work are appropriately investigated and resolved: AN, TO and KH.

Dr. Alhusain Nagm, MD, MSc, the corresponding author of this article contained within the original manuscript which includes any diagrams and photographs and any related or stand-alone film submitted (the Contribution) has the right to grant on behalf of all authors.

## Conflicts of Interest Disclosure

The authors have no personal, financial, or institutional interest in any of the drugs, materials, or devices

in the article. All authors who are members of the Japan Neurosurgical Society (JNS) have registered online Self-reporting Conflict Disclosure Statement Forms through the website for JNS members.

## References

- 1) Gardner PA, Bergsneider M, Harvey RJ, et al.: Endoscopic Series 1 of 7: Introduction to Endoscopic Endonasal Surgery, 2017. Available from: <http://learn.cns.org/diweb/catalog/item/id/1096452> (accessed 3 Jan, 2018)
- 2) Gardner PA, Sorenson JM, Heilman CB, et al.: Endoscopic Series 2 of 7: Pituitary Tumors and CSF Leaks, 2017. Available from: <http://learn.cns.org/diweb/catalog/item/id/1332165> (accessed 3 Jan, 2018)
- 3) Gardner PA, Prevedello D, Sorenson JM, et al.: Endoscopic Series 3 of 7: Transclival/Transodontoid Approaches, 2017. Available from: <http://learn.cns.org/diweb/catalog/item/id/1447859> (accessed 3 Jan, 2018)
- 4) Gardner PA, Sorenson JM, Sindwani R, et al.: Endoscopic Series 4 of 7: Suprasellar/Transplanum Approaches, 2017. Available from: <http://learn.cns.org/diweb/catalog/item/id/1538335> (accessed 3 Jan, 2018)
- 5) Gardner PA, Fernandez-Miranda JC, Casiano R, et al.: Endoscopic Series 5 of 7: Endoscopic Endonasal Transcribriform Approaches, 2017. Available from: <http://learn.cns.org/diweb/catalog/item/id/1600787> (accessed 3 Jan, 2018)
- 6) Gardner PA, Bendok BR, Carrau R, et al.: Endoscopic Series 6 of 7: Coronal Plane/Vascular Surgery, 2017. Available from: <http://learn.cns.org/diweb/catalog/item/id/1628475> (accessed 3 Jan, 2018)
- 7) Gardner PA, Carrau R, Snyderman CH, et al.: Endoscopic Series 7 of 7: Endonasal Skull Base Reconstruction, 2017. Available from: <http://learn.cns.org/diweb/catalog/item/id/1683518> (accessed 3 Jan, 2018)
- 8) Koutourosiou M, Fernandez-Miranda JC, Vaz-Guimaraes Filho F, et al.: Outcomes of endonasal and lateral approaches to petroclival meningiomas. *World Neurosurg* 99: 500–517, 2017
- 9) Koutourosiou M, Gardner PA, Tormenti MJ, et al.: Endoscopic endonasal approach for resection of cranial base chordomas: outcomes and learning curve. *Neurosurgery* 71: 614–624; discussion 624–625, 2012
- 10) Koutourosiou M, Filho FV, Costacou T, et al.: Pontine encephalocele and abnormalities of the posterior fossa following transclival endoscopic endonasal surgery. *J Neurosurg* 121: 359–366, 2014
- 11) Pinheiro-Neto CD, Paluzzi A, Fernandez-Miranda JC, et al.: Extended dissection of the septal flap pedicle for ipsilateral endoscopic transpterygoid approaches. *Laryngoscope* 124: 391–396, 2014
- 12) Koutourosiou M, Fernandez-Miranda JC, Wang EW, Snyderman CH, Gardner PA: Endoscopic endonasal



- surgery for olfactory groove meningiomas: outcomes and limitations in 50 patients. *Neurosurg Focus* 37: E8, 2014
- 13) Cappabianca P, Cavallo LM, Valente V, et al.: Sellar repair with fibrin sealant and collagen fleece after endoscopic endonasal transsphenoidal surgery. *Surg Neurol* 62: 227–233, 2004
  - 14) Fraser S, Gardner PA, Koutourousiou M, et al.: Risk factors associated with postoperative cerebrospinal fluid leak after endoscopic endonasal skull base surgery. *J Neurosurg* 128: 1066–1071, 2018
  - 15) Hadad G, Bassagasteguy L, Carrau RL, et al.: A novel reconstructive technique after endoscopic expanded endonasal approaches: vascular pedicle nasoseptal flap. *Laryngoscope* 116: 1882–1886, 2006
  - 16) Kobayashi S, Hara H, Okudera H, Takemae T, Sugita K: Usefulness of ceramic implants in neurosurgery. *Neurosurgery* 21: 751–755, 1987
  - 17) Luginbuhl AJ, Campbell PG, Evans J, Rosen M: Endoscopic repair of high-flow cranial base defects using a bilayer button. *Laryngoscope* 120: 876–880, 2010
  - 18) Yano S, Tsuiki H, Kudo M, et al.: Sellar repair with resorbable polyglactin acid sheet and fibrin glue in endoscopic endonasal transsphenoidal surgery. *Surg Neurol* 67: 59–64, 2007
  - 19) Fortes FS, Carrau RL, Snyderman CH, et al.: Transpterygoid transposition of a temporoparietal fascia flap: a new method for skull base reconstruction after endoscopic expanded endonasal approaches. *Laryngoscope* 117: 970–976, 2007
  - 20) Patel MR, Shah RN, Snyderman CH, et al.: Pericranial flap for endoscopic anterior skull-base reconstruction: clinical outcomes and radioanatomic analysis of preoperative planning. *Neurosurgery* 66: 506–512, 2010
  - 21) Ivan ME, Iorgulescu JB, El-Sayed I, et al.: Risk factors for postoperative cerebrospinal fluid leak and meningitis after expanded endoscopic endonasal surgery. *J Clin Neurosci* 22: 48–54, 2015
  - 22) Esposito F, Dusick JR, Fatemi N, Kelly DF: Graded repair of cranial base defects and cerebrospinal fluid leaks in transsphenoidal surgery. *Neurosurgery* 60: 295–303; discussion 303–304, 2007
  - 23) Fortes FS, Carrau RL, Snyderman CH, et al.: The posterior pedicle inferior turbinate flap: a new vascularized flap for skull base reconstruction. *Laryngoscope* 117: 1329–1332, 2007
  - 24) Harvey RJ, Parmar P, Sacks R, Zanation AM: Endoscopic skull base reconstruction of large dural defects: a systematic review of published evidence. *Laryngoscope* 122: 452–459, 2012
  - 25) Hida K, Yamaguchi S, Seki T, et al.: Nonsuture dural repair using polyglycolic acid mesh and fibrin glue: clinical application to spinal surgery. *Surg Neurol* 65: 136–142; discussion 142–143, 2006
  - 26) Ogiwara T, Goto T, Nagm A, Hongo K: Endoscopic endonasal transsphenoidal surgery using the iArmS operation support robot: initial experience in 43 patients. *Neurosurg Focus* 42: E10, 2017
  - 27) Ogiwara T, Nagm A, Yamamoto Y, Hasegawa T, Nishikawa A, Hongo K: Clinical characteristics of pituitary adenomas with radiological calcification. *Acta Neurochir (Wien)* 159: 2187–2192, 2017
  - 28) Oshino S, Saitoh Y, Yoshimine T: Withstand pressure of a simple fibrin glue sealant: experimental study of mimicked sellar reconstruction in extended transsphenoidal surgery. *World Neurosurg* 73: 701–704, 2010
  - 29) Sigler AC, D’Anza B, Lobo BC, Woodard TD, Recinos PF, Sindwani R: Endoscopic skull base reconstruction: an evolution of materials and methods. *Otolaryngol Clin North Am* 50: 643–653, 2017
  - 30) Snyderman C, Kassam A, Carrau R, Mintz A, Gardner P, Prevedello DM: Acquisition of surgical skills for endonasal skull base surgery: a training program. *Laryngoscope* 117: 699–705, 2007
  - 31) Snyderman CH, Fernandez-Miranda J, Gardner PA: Training in neurosinology: the impact of case volume on the learning curve. *Otolaryngol Clin North Am* 44: 1223–1228, 2011
  - 32) Canuto RA, Pol R, Martinasso G, Muzio G, Gallesio G, Mozzati M: Hydroxyapatite paste Ostim, without elevation of full-thickness flaps, improves alveolar healing stimulating BMP- and VEGF-mediated signal pathways: an experimental study in humans. *Clin Oral Implants Res* 24 Suppl A100: 42–48, 2013
  - 33) Kaneko TS, Sehgal V, Skinner HB, et al.: Radioactive bone cement for the treatment of spinal metastases: a dosimetric analysis of simulated clinical scenarios. *Phys Med Biol* 57: 4387–4401, 2012
  - 34) Pugh LR, Clarkson PW, Phillips AE, Biau DJ, Masri BA: Tumor endoprosthesis revision rates increase with peri-operative chemotherapy but are reduced with the use of cemented implant fixation. *J Arthroplasty* 29: 1418–1422, 2014
  - 35) Vorndran E, Geffers M, Ewald A, Lemm M, Nies B, Gbureck U: Ready-to-use injectable calcium phosphate bone cement paste as drug carrier. *Acta Biomater* 9: 9558–9567, 2013
  - 36) Zou W, Chen X: Osteogenesis and ototoxicity of a novel preparation of autogenous bone cement: implications for mastoid obliteration. *Otolaryngol Head Neck Surg* 151: 1020–1027, 2014
  - 37) Nagm A, Ogiwara T, Goto T, Chiba A, Hongo K: Neuroendoscopy via an extremely narrow foramen of Monro: a case report. *NMC Case Rep J* 4: 37–42, 2016
  - 38) Mori K: Dissectable modified three-dimensional temporal bone and whole skull base models for training in skull base approaches. *Skull Base* 19: 333–343, 2009
  - 39) Narayanan V, Narayanan P, Rajagopalan R, et al.: Endoscopic skull base training using 3D printed models with pre-existing pathology. *Eur Arch Otorhinolaryngol* 272: 753–757, 2015

- 40) Snyderman CH, Gardner PA, Fernandez-Miranda J, Wang EW: Anatomical Dissection Guide: Pittsburgh Comprehensive Course. UPMC Comprehensive Endoscopic Endonasal Surgery, 2018. Available from: <https://treatspace.com/practice/the-skull-base-congress/resources/pittsburgh-course/anatomical-dissection-guide-pittsburgh-comprehensive-course> (accessed 2 Jan, 2018)
- 41) Inoue M, Sakane M, Taguchi T: Fabrication of reactive poly(vinyl alcohol) membranes for prevention of bone cement leakage. *J Biomed Mater Res B Appl Biomater* 102: 1786–1791, 2014
- 42) Lukaszczyk J, Janicki B, López A, et al.: Novel injectable biomaterials for bone augmentation based on isosorbide dimethacrylic monomers. *Mater Sci Eng C Mater Biol Appl* 40: 76–84, 2014

---

*Address reprint requests to:* Alhusain Nagm, MD, MSc,  
Department of Neurosurgery, Shinshu University  
School of Medicine, 3-1-1 Asahi, Matsumoto, Nagano  
390-8621, Japan.  
*e-mail:* nagm@shinshu-u.ac.jp